



HAL
open science

Refining Viscous and Thermal Dynamic Tortuosities for Highly Resistive Porous Materials: A Theoretical and Experimental Investigation

Abdellah Bouchendouka, Zine El Abiddine Fellah, Denis Lafarge, Thierry Scotti, Erick Ogam, Camille Perrot, Claude L. Depollier

► To cite this version:

Abdellah Bouchendouka, Zine El Abiddine Fellah, Denis Lafarge, Thierry Scotti, Erick Ogam, et al.. Refining Viscous and Thermal Dynamic Tortuosities for Highly Resistive Porous Materials: A Theoretical and Experimental Investigation. CFA 2025 - 17e Congrès Français d'Acoustique, Apr 2025, Paris, France. <hal-05219889>

HAL Id: hal-05219889

<https://hal.science/hal-05219889v1>

Submitted on 22 Aug 2025

HAL is a multi-disciplinary open access archive for the deposit and dissemination of scientific research documents, whether they are published or not. The documents may come from teaching and research institutions in France or abroad, or from public or private research centers.

L'archive ouverte pluridisciplinaire HAL, est destinée au dépôt et à la diffusion de documents scientifiques de niveau recherche, publiés ou non, émanant des établissements d'enseignement et de recherche français ou étrangers, des laboratoires publics ou privés.



HAL Authorization



17^e Congrès Français d'Acoustique
27-30 avril 2025, Paris

Refining Viscous and Thermal Dynamic Tortuosities for Highly Resistive Porous Materials: A Theoretical and Experimental Investigation

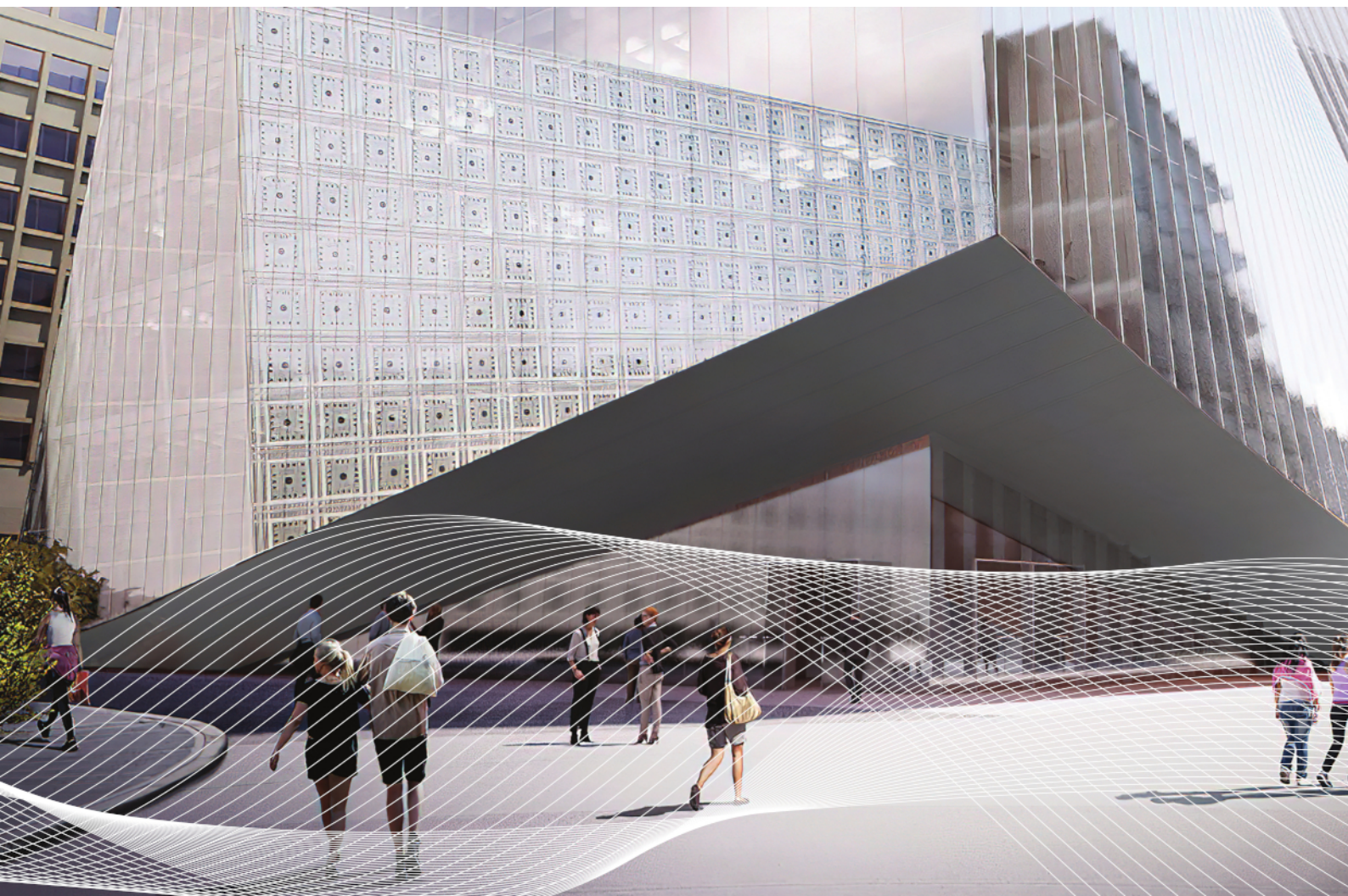
A. Bouchendouka¹, Z. E. A. Fellah¹, D. Lafarge², T. Scotti¹, E. Ogam¹, C. Perrot³, and C. Depollier⁴

¹*Aix Marseille Univ, CNRS, Centrale Med, LMA, Marseille, France*

²*Laboratoire d'Acoustique de l'Université du Mans, UMR 6613, 72085 Le Mans, France*

³*Univ Gustave Eiffel, Univ Paris Est Creteil, CNRS, UMR 8208, MSME, F-77454 Marne-la-Vallée, France*

⁴*Acoustics Laboratory of the University of Le Mans (LAUM), UMR 6613, Institut d'Acoustique -Graduate School (IA-GS), CNRS, Le Mans University, Le Mans, France*



The accurate prediction of wave propagation in highly resistive porous materials requires refined descriptions of visco-thermal interactions. Recently, new effective pore sizes Σ , Σ' , V , and V' were introduced in the expansion of the Johnson-Champoux-Allard (JCA) dynamic tortuosities $\alpha(\omega)$ and $\alpha'(\omega)$, significantly improving the agreement between theoretical models and ultrasonic transmission experiments. In this work, we investigate the microscopic wave propagation problem in cylindrical pores to provide a physical interpretation of these higher-order parameters. By analyzing the velocity profile inside the pore in the high-frequency regime, we demonstrate that the classical JCA characteristic lengths Λ , Λ' may be insufficient for porous media with non-trivial connectivity, where visco-thermal interactions require a more refined treatment. Experimental validations are conducted using ultrasonic transmission measurements on highly resistive plastic foams in the 70–130 kHz range, confirming the necessity of including V and V' in the expansion of the dynamic tortuosity. These findings provide crucial insights into the complex physics of visco-thermal interactions and offer an extension to the JCA model, enabling the characterization of a broader class of porous materials with intricate microstructures. The proposed approach has potential applications in optimizing sound-absorbing materials for industrial and engineering applications.

1 Introduction

Recently, new effective pore sizes Σ , Σ' , V , and V' were introduced in [1] in the Johnson-Champoux-Allard [2, 3] dynamic tortuosities $\alpha(\omega)$ and $\alpha'(\omega)$ to enhance the prediction of ultrasonic transmitted waves by highly resistive porous samples. More specifically, it was demonstrated that the parameter V (and its thermal counterpart V') has a special significance, where a good agreement between experiment and theory is achievable only when including this term in the expansion of the dynamic tortuosity. Nevertheless, the general definition of these parameters is not a simple task and is still an ongoing investigation. For this reason, we first investigate the microscopic problem describing wave propagation in cylindrical pores, and provide a definition for these terms in such geometry to gain an initial understanding. Moreover, we conduct experimental measurements of the different parameters using transmitted spectra by highly resistive plastic foams in the 70-130 kHz frequency range. The agreement between experiment and theory using the higher order terms is remarkably good. We end this paper by an overall conclusion of the results obtained.

2 Context

The fundamental equations that describe wave propagation in a fluid with density ρ_f and bulk modulus K_f are Euler equations, which are written as:

$$i\omega\rho_f v = -\partial_x p, \quad i\omega\frac{p}{K_f} = -\partial_x v \quad (1)$$

where v is the fluid velocity, p the pressure, ω the angular frequency, and $i = \sqrt{-1}$. If we consider the fluid motion to be limited by an arbitrary geometry in a porous medium, visco-inertial and thermal effects must be introduced because of the interaction between the fluid and the solid frame. This means that the fluid properties ρ_f and K_f become linear functions $\rho(\omega) = \rho_f \alpha(\omega)$ and $K(\omega) = K_f (\gamma - (\gamma - 1) / \alpha'(\omega))^{-1}$ that take into account these effects. The response functions $\alpha(\omega)$ and $\alpha'(\omega)$ are called the viscous and thermal dynamic tortuosities, respectively, which are a natural result of the homogenization process of the microscopic problem that

describes fluid motion at a pore scale. Euler equations in the case of wave propagation in a porous medium take the following form:

$$i\omega\rho_f \alpha(\omega) \langle v \rangle = -\partial_x \langle p \rangle, \quad i\omega \left(\gamma - \frac{\gamma - 1}{\alpha'(\omega)} \right) \frac{\langle p \rangle}{K_f} = -\partial_x \langle v \rangle \quad (2)$$

where $\langle \rangle$ is the pore volume average operator, and γ the adiabatic index. In this paper we are more interested in the high frequency regime, where the response functions are given by:

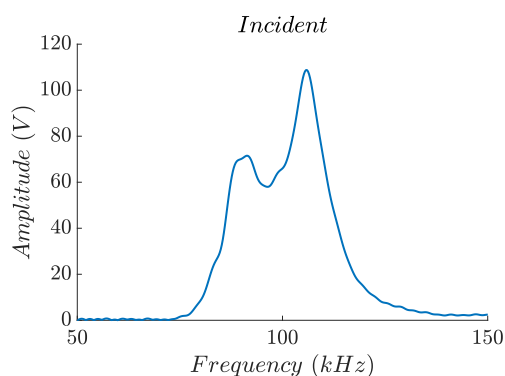


Figure 1: Measured incident spectrum

$$\alpha(\omega) = \alpha_\infty \left(1 + \frac{2}{\Lambda} \varepsilon(\omega) + O(\varepsilon(\omega)^2) \right), \quad (3)$$

$$\alpha'(\omega) = \alpha'_\infty \left(1 + \frac{2}{\Lambda'} \varepsilon'(\omega) + O(\varepsilon'(\omega)^2) \right), \quad (4)$$

where α_∞ is the ideal fluid tortuosity, $\alpha'_\infty = 1$ is the thermal tortuosity. The JCA model disregards the precise remaining terms in this asymptotics and relies only on two characteristic sizes, namely the viscous characteristic length Λ , and the thermal characteristic length Λ' . The terms $\varepsilon(\omega) = \sqrt{\nu/(i\omega)}$, and $\varepsilon'(\omega) = \varepsilon(P_r, \omega)$ are called the complex viscous and thermal skin depths, respectively, with ν being the kinematic viscosity, and P_r the Prandtl number.

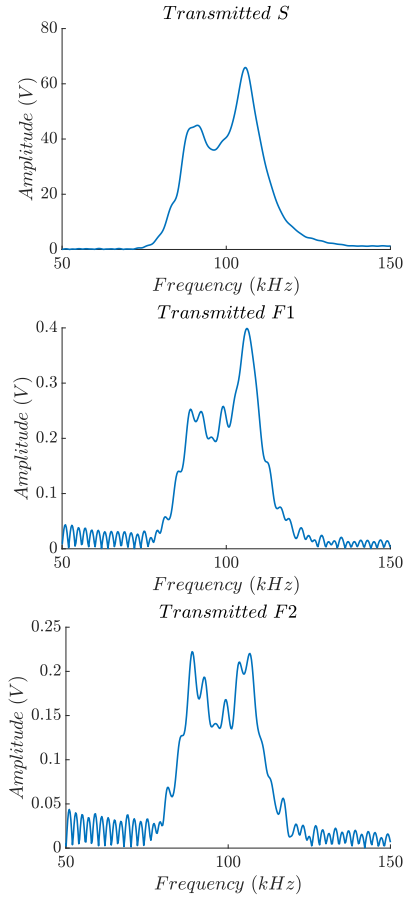


Figure 2: Measured transmitted spectra by foams S , $F1$ and $F2$.

It was demonstrated recently in [1] that the JCA model struggles with predicting the experimental transmitted signal of certain plastic foams. These foams are used for noise reduction in the automotive industry (refer to [4] for more details), possessing highly resistive characteristics, where a 99% reduction in transmitted signal amplitude was observed. This unusual attenuation is tied to a significant increase in the visco-thermal dissipation that could not be captured accurately considering only the lengths Λ and Λ' . To tackle this issue, Bouchendouka *et al.* [1] proposed the following:

$$\alpha(\omega) = \alpha_\infty \left(1 + \frac{2}{\Lambda} \varepsilon(\omega) + \frac{3}{\Sigma} \varepsilon(\omega)^2 + \frac{a}{V} \varepsilon(\omega)^3 \right), \quad (5)$$

$$\alpha'(\omega) = \alpha'_\infty \left(1 + \frac{2}{\Lambda'} \varepsilon'(\omega) + \frac{3}{\Sigma'} \varepsilon'(\omega)^2 + \frac{a}{V'} \varepsilon'(\omega)^3 \right), \quad (6)$$

where Σ , Σ' are effective surfaces, and V , V' are effective volumes. Eqs.(5)-(6) were shown to give a very good agreement between experiment and theory (see refs [1]). Surprisingly, this agreement is achievable only when including the fourth order terms ε^3/V and ε'^3/V' . It is important to note that the existence of an expansion in the response functions was already known in the literature [5, 6, 7, 8], but its significance in capturing very complex visco-thermal effects was only demonstrated recently in [1].

The underlying physics behind the expansion of $\alpha(\omega)$ and $\alpha'(\omega)$ will be discussed in the next sections.

3 Wave propagation in cylindrical pores

It is well known [9] that the dynamic tortuosities in cylindrical pores with radius R have the following expressions:

$$\alpha(\omega) = \left[1 - \frac{2}{s \sqrt{-j}} \frac{J_1(s \sqrt{-j})}{J_0(s \sqrt{-j})} \right]^{-1}, \quad (7)$$

$$\alpha'(\omega) = \alpha(P_r, \omega), \quad (8)$$

$$(9)$$

where J_1 and J_0 are the first and zeroth order Bessel functions of the first kind respectively, and $s = R \sqrt{\omega/\nu}$. In order to determine the expansion of these functions in the high frequency limit, we use the large argument Hankel's asymptotic expansion for J_1 and J_0 (see Eq.(9.2.5) in ref [10]), then it is easy to show that the response function can be written as:

$$\alpha(\omega) = 1 + \frac{\sum_{k \geq 0} \Upsilon_k \left(\left(\frac{\varepsilon}{R} \right)^{2k+1} \Phi_{k,1} - \left(\frac{\varepsilon}{R} \right)^{2k+2} \Phi_{k,2} \right)}{\sum_{k \geq 0} \Upsilon_k \left(\left(\frac{\varepsilon}{R} \right)^{2k} + \left(\frac{\varepsilon}{R} \right)^{2k+1} \Phi_{k,3} + \left(\frac{\varepsilon}{R} \right)^{2k+2} \Phi_{k,2} \right)} \quad (10)$$

where

$$\begin{aligned} \Upsilon_k &= \frac{(4k)!^2}{2^{10k} (2k)!^3}, & \Phi_{k,1} &= -2 \frac{(4k+1)}{(4k-1)}, \\ \Phi_{k,2} &= \frac{(4k+1)(4k+3)}{2(4k+2)}, & \Phi_{k,3} &= \frac{(4k+1)(4k+3)(4k+5)}{4(4k-1)(4k+2)} \end{aligned} \quad (11)$$

If we want to obtain the coefficients until the fourth order term, we will have to set $k = 1$ in the summation, and by performing simple Polynomial division we get the following:

$$\alpha(\omega) = 1 + 2 \frac{\varepsilon(\omega)}{R} + 3 \frac{\varepsilon(\omega)^2}{R^2} + \frac{15}{4} \frac{\varepsilon(\omega)^3}{R^3}, \quad (12)$$

$$\alpha'(\omega) = 1 + 2 \frac{\varepsilon'(\omega)}{R} + 3 \frac{\varepsilon'(\omega)^2}{R^2} + \frac{15}{4} \frac{\varepsilon'(\omega)^3}{R^3} \quad (13)$$

Following Johnson *et al.* [2], we choose to define the different parameters in cylindrical pores as:

$$\Lambda' = \Lambda = R, \quad \Sigma' = \Sigma = R^2, \quad V' = V = R^3. \quad (14)$$

Therefore, the constant a in Eqs.(5)-(6) is chosen to be 15/4 based on these calculations.

4 Experimental measurements

In this section we wish to demonstrate the significance of the higher order terms Σ and V (and their thermal

counterparts) experimentally. The experimental setup consists of two Ultratransducers of central frequency of 100 kHz, one acting as an emitter, and the other one as a receiver. We use plastic foams as porous specimens, which are placed in between these transducers in order to measure the transmission data (signal or spectrum) by these foams, where the measurements are done in air. The setup also consists of a pulse generator, and a digital oscilloscope to visualize the experimental data (see Ref [1] for more details on the experimental setup). The foam specimens we used, denoted $F1$ and $F2$ (thicknesses: 2 cm, 2.5 cm), are highly resistive foams fabricated with graphite particles to enhance fire resistance, showed altered pore size distribution and increased structural heterogeneity. We use another ordinary foam denoted as S with thickness 1.4 cm, with relatively moderate resistive characteristics compared to the highly resistive foams $F1$ and $F2$. In Ref [1] the experimental measurements were done using temporal signals, however, in this paper we wish to do the measurements using spectra to gain further insights about the significance of the terms Σ and V .

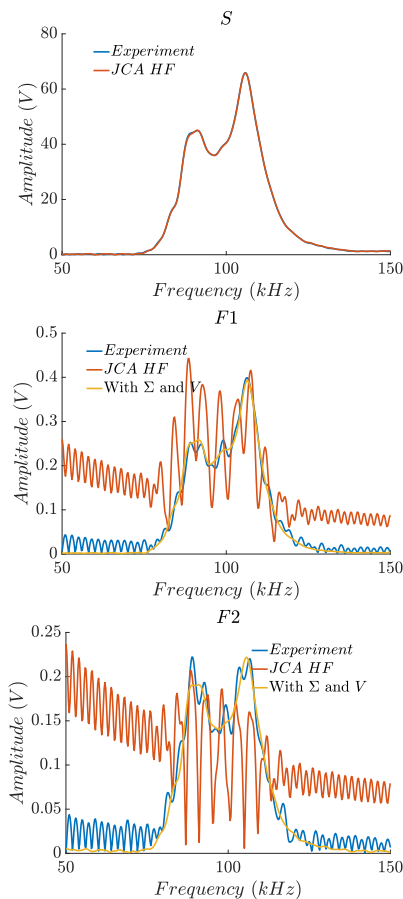


Figure 3: Comparison of the measured transmitted spectrum (blue line) with theoretical signals generated using the JCA high-frequency model (red line) and the extended model incorporating Σ and V (yellow line) for foams S , $F1$ and $F2$.

Figure 1 represents the experimental incident spectrum.

From this figure, we can see that the experimental measurements are conducted mainly in the 70-130 kHz frequency range. Figure 2 shows the transmitted spectra by foams S , $F1$, and $F2$. Interestingly, the energy loss by foams $F1$ and $F2$ is significantly higher than that of S . For example, if one uses the peak amplitude of the incident spectrum $A_{peak}^{incident}$, as a reference value to estimate the energy loss, we get:

$$E_{ratio}^S = \frac{[A_{peak}^S]^2}{[A_{peak}^{incident}]^2} \times 100 \approx 35\% \quad (15)$$

$$E_{ratio}^{F1} = \frac{[A_{peak}^{F1}]^2}{[A_{peak}^{incident}]^2} \times 100 \approx 0.0011\% \quad (16)$$

$$E_{ratio}^{F2} = \frac{[A_{peak}^{F2}]^2}{[A_{peak}^{incident}]^2} \times 100 \approx 0.00036\%. \quad (17)$$

This demonstrates the significant energy loss by foams $F1$ and $F2$ compared with S , where 35 % of energy is transmitted by S , whereas only 0.0011% and 0.00036% of energy is transmitted by foams $F1$ and $F2$, respectively. This means that these foams possess excellent sound absorbing qualities. Nevertheless, theoretical modeling is crucial if one wants to understand the physics behind this significant attenuation, enhance acoustic performance, and design optimization. The most known model used in the literature is the Johnson-Champoux-Allard model represented by Eqs.(3)-(4). We want to employ it to characterize these foams, as well as with the extended modeling proposed in [1] and represented by Eqs.(5)-(6).

Figure 3 represents a comparison between experimental measurements and theoretical predictions for the three foam specimens. In particular, for foam S , a very good match between experiment (blue) and the prediction by JCA model (red) is observed. This is expected because of the moderate attenuation of this foam, which signifies that the underlying cause behind this energy loss is simple viscous and thermal boundary layer effects which are well described by JCA. On the other hand, the basic JCA model overestimates the transmitted amplitude of foams $F1$, $F2$ in certain frequency regions, showing pronounced resonances and failing to align well with the experimental peak. By contrast, the extended model (yellow) tracks the measured spectrum more closely across the entire 50–150 kHz band: it captures both the rise toward the main peak around 100 kHz and the subsequent roll-off with fewer discrepancies. Therefore, a good match is achieved only when including Σ and V . The experimental results for the different parameters are summarized in Table 1.

Before we discuss the physical significance of Σ and V , let's first understand what are the physics governing this substantial energy dissipation. Generally speaking, visco-thermal effects are the primary cause of acoustic energy loss in porous materials. Accordingly, these can depend on the pore morphology, pore surface roughness or

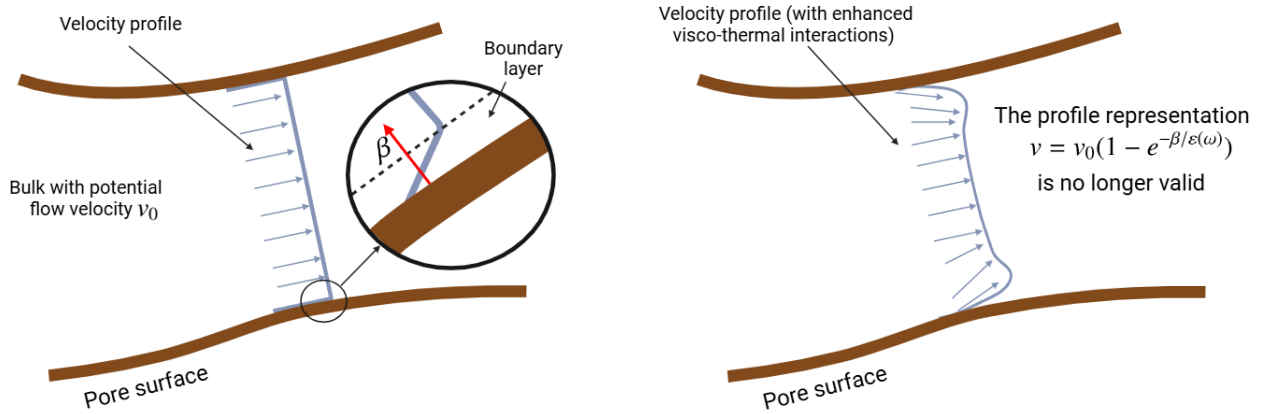


Figure 4: Representation of the velocity profile inside a pore in the high frequency regime, (left) velocity represented by the profile (18), (right) velocity profile with enhanced visco-thermal effects which are not captured by Eq.(18)

curvature, and complex pore space connectivity. Another reason is scattering. In particular if scattering dominates, then the expansions used here are not physically justified. Nevertheless, the ratio λ/\bar{R} ranges from 10 to 16 over the 70-130 kHz frequency bandwidth considered in this study (with λ being the wavelength), assuming an average pore size $\bar{R} = 300 \mu\text{m}$ [4]. While small scattering effects may exist, visco-thermal losses remain the dominant source of attenuation. In this regard, it is easy to understand that Σ and V (and Σ' , V') capture more complex visco-thermal interactions not captured by Λ , Λ' alone. These complex mechanisms are not tied only to surface effects, but effects that appear deeper inside the pore. It is widely known that Λ is defined via the exponential decay of the velocity profile near the pore walls, where the velocity in the general case is written as:

$$v = v_0(1 - e^{-\beta/\epsilon(\omega)}), \quad (18)$$

where v_0 is the potential flow velocity, β a coordinate normal to the pore surface pointing inside the bulk. However, the representation (18) is too simple, and does not give us any information about pore roughness, curvature, or the complexity of the geometry in general (see figure 4). Therefore, when accounting for more complex visco-thermal interactions Eq.(18) will have a quite different expression with additional higher order terms directly linked to Σ and V . The general definition of these terms is currently under investigation and will be published elsewhere.

5 Conclusion

In conclusion, we have demonstrated the importance of considering the expansion of the dynamic tortuosities $\alpha(\omega)$ and $\alpha(\omega)'$ by including the higher order terms Σ , Σ' , V , V' . Porous samples with non-trivial pore connectivity enhance visco-thermal interactions, where the Johnson-Champoux-Allard terms Λ , Λ' are not sufficient enough to handle such complexity. Indeed, these terms are linked to a

| <i>Samples</i> | S | F1 | F2 |
|------------------------------|-------------|-----------------------|-----------------------|
| <i>Model used</i> | JCA | with Σ and V | with Σ and V |
| ϕ | ≈ 1 | ≈ 1 | ≈ 1 |
| α_∞ | 1,028 | 1,17 | 1,13 |
| Λ (μm) | 214,71 | 42.75 | 37,89 |
| Σ (μm^2) | / | 2916 | 5285 |
| V (μm^3) | / | 3916 | 7163 |

Table 1: Summary of the results obtained for the different foam specimens.

simple exponential decay of the velocity profile inside the pore in the high frequency regime. However, for certain porous samples with complex visco-thermal interactions, the exponential decay representation is not valid, and refinements of the profile in the general case are required to obtain a general definition of the high order terms.

These results are of paramount importance for understanding complex visco-thermal physics. Moreover, the proposed modeling approach can be used as an extension to JCA model to characterize a wider range of porous materials with complex geometries, which is useful in enhancing sound absorption properties for multiple industrial applications.

References

- [1] A. Bouchendouka, Improving acoustic wave propagation models in highly attenuating porous materials, *The Journal of the Acoustical Society of America* **155**, 206-217 (2024).
- [2] D. L. Johnson, J. Koplik, R. Dashen, Theory of dynamic permeability and tortuosity in fluid-saturated porous media, *Journal of fluid mechanics* **176**, 379-402 (1987).
- [3] Y. Champoux, J. F. Allard, Dynamic tortuosity and bulk modulus in air-saturated porous media, *Journal of applied physics* **70**, 1975-1979 (1991).
- [4] C. T. Nguyen, Acoustic foams with pore size distributions and controlled interconnections: Relationships between

- structures, properties, fabrication, Ph.D. thesis, *Université Gustave Eiffel* (2021).
- [5] J. Kergomard, D. Lafarge, and J. Gilbert, Transients in porous media: Exact and modelled time-domain Green's functions, *Acta Acustica united with Acustica* **99**(4), 557–571 (2013).
- [6] R. Roncen, Z. E. A. Fellah, E. Piot, F. Simon, E. Ogam, M. Fellah, and C. Depollier, Inverse identification of a higher order viscous parameter of rigid porous media in the high-frequency domain, *The Journal of the Acoustical Society of America* **145**(3), 1629–1639 (2019).
- [7] D. Lafarge, Acoustic wave propagation in viscothermal fluids, in *Acoustic Waves in Periodic Structures, Metamaterials, and Porous Media*, edited by N. Jimenez, O. Umnova, and J.-P. Groby, Springer, pp. 205–272 (2021).
- [8] D. Lafarge, Nonlocal dynamic homogenization of fluid-saturated metamaterials, in *Acoustic Waves in Periodic Structures, Metamaterials, and Porous Media*, edited by N. Jimenez, O. Umnova, and J.-P. Groby, Springer, pp. 273–331 (2021).
- [9] J. Allard and N. Atalla, *Propagation of Sound in Porous Media: Modelling Sound Absorbing Materials*, John Wiley & Sons (2009).
- [10] M. Abramowitz, I. A. Stegun, *Handbook of mathematical functions with formulas, graphs, and mathematical tables*, *The Journal of the Acoustical Society of America*, US Government printing office (1968).